Ab initio study of nitrogen and position-specific oxygen kinetic isotope effects in the NO + O$_3$ reaction

Wendell W. Walters and Greg Michalski

Ab initio study of nitrogen and position-specific oxygen kinetic isotope effects in the NO + O$_3$ reaction

Wendell W. Walters[1,a)] and Greg Michalski[1,2]

[1]*Department of Earth, Atmospheric, and Planetary Sciences Purdue University, 550 Stadium Mall Drive, West Lafayette, Indiana 47907, USA*
[2]*Purdue University, 560 Oval Drive, West Lafayette, Indiana 47907, USA*

Ab initio calculations have been carried out to investigate nitrogen (k^{15}/k^{14}) and position-specific oxygen (k^{17}/k^{16}O & k^{18}/k^{16}) kinetic isotope effects (KIEs) for the reaction between NO and O$_3$ using CCSD(T)/6-31G(d) and CCSD(T)/6-311G(d) derived frequencies in the complete Bigeleisen equations. Isotopic enrichment factors are calculated to be −6.7‰, −1.3‰, −44.7‰, −14.1‰, and −0.3‰ at 298 K for the reactions involving the ^{15}N^{16}O, ^{14}N^{18}O, ^{18}O^{16}O^{16}O, ^{16}O^{18}O^{16}O, and ^{16}O^{16}O^{18}O isotopologues relative to the 14N^{16}O and 16O$_3$ isotopologues, respectively (CCSD(T)/6-311G(d)). Using our oxygen position-specific KIEs, a kinetic model was constructed using *Kintecus*, which estimates the overall isotopic enrichment factors associated with unreacted O$_3$ and the oxygen transferred to NO$_2$ to be −19.6‰ and −22.8‰, respectively, (CCSD(T)/ 6-311G(d)) which tends to be in agreement with previously reported experimental data. While this result may be fortuitous, this agreement suggests that our model is capturing the most important features of the underlying physics of the KIE associated with this reaction (i.e., shifts in zero-point energies). The calculated KIEs will useful in future NO$_x$ isotopic modeling studies aimed at understanding the processes responsible for the observed tropospheric isotopic variations of NO$_x$ as well as for tropospheric nitrate. *Published by AIP Publishing.* [http://dx.doi.org/10.1063/1.4968562]

I. INTRODUCTION

Nitrogen oxides (NO$_x$ = NO + NO$_2$) are important trace gases that influence the concentrations of atmospheric oxidants that drive tropospheric and stratospheric chemistry.[1–4] During the daytime, NO$_x$ exists in a closed photochemical cycle between NO–O$_2$–O$_3$–NO$_2$ in the atmosphere, known as the Leighton cycle.[1,5] This cycle is initiated when NO$_2$ is photolyzed by UV-visible light in the blue region of the spectrum (<400 nm) yielding O(^{3}P) the ground state of the oxygen atom. This liberated oxygen atom can combine with O$_2$ to form O$_3$, which then oxidizes NO back to NO$_2$,[1,5]

$$NO_2 + h\nu \rightarrow NO + O\,(^3P), \tag{R1}$$

$$O(^3P) + O_2 \rightarrow {}^*O_3, \tag{R2}$$

$${}^*O_3 + M \rightarrow O_3 + M^*, \tag{R3}$$

$$O_3 + NO \rightarrow NO_2 + O_2. \tag{R4}$$
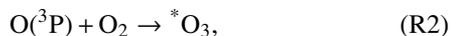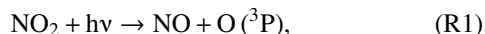
The analysis of the oxygen and nitrogen stable isotopes of NO$_x$ and its oxidation product, atmospheric nitrate, may help in our understanding of this photochemical cycling[6–10] and sources of NO$_x$.[11–13] Variations in oxygen and nitrogen isotope compositions are reported using δ(‰) notation where δ^{x}O(‰) and δ^{15}N(‰) = (R$_{sample}$/R$_{ref}$ − 1) × 1000, where R$_{sample}$ and R$_{ref}$ denote the ^{x}O/^{16}O (x = 17 or 18) or ^{15}N/^{14}N in the sample or reference, respectively. The oxygen isotopic reference is Vienna Standard Mean Ocean Water

(VSMOW) and the nitrogen isotopic reference is atmospheric air. However, δ^{18}O and δ^{15}N of NO$_x$ may also be influenced by isotopic fractionation processes associated with the Leighton cycle ((R1)–(R4)),[14,15] which may be propagated into atmospheric nitrate,[16] yet few of these fractionation factors have been determined.

The photochemical cycling of NO$_x$ is rapid, and prior experimental investigations of this cycling have suggested that isotopic equilibrium is achieved between O$_3$ and NO$_x$, erasing any original O isotopic NO$_x$ signatures.[10] Several studies have shown that atmospheric O$_3$ has an elevated δ^{18}O and a strong mass-independent component that is quantified by Δ^{17}O notation,[17–22]

$$\Delta^{17}O(‰) = 1000 \ln\left[1 + \frac{\delta^{17}O}{1000}\right] - \lambda \times 1000 \ln\left[1 + \frac{\delta^{18}O}{1000}\right]. \tag{1}$$

In Eq. (1) the λ is mass-dependent coefficient, which may be approximated as 0.52.[23] During the photochemical cycling of NO$_x$, these elevated δ^{18}O and Δ^{17}O signatures of O$_3$ are transferred to NO$_x$ as a result of (R4).[8,10,24] While Δ^{17}O of the transferred O atom from O$_3$ to NO$_2$ should be minimally impacted, δ^{18}O may be significantly altered as a result of the mass-dependent fractionation associated with the kinetic isotope effect (KIE) of (R4). Thus, the kinetic isotope effect associated with (R4) may play an important role in the δ^{18}O of NO$_x$, which may be propagated into atmospheric nitrate, yet this fractionation factor is relatively unknown. Post-deposition isotope effects of nitrate such as photolysis of nitrate in a particle may alter the isotopic composition of

a)Electronic mail: waltersw@purdue.edu

nitrate,[25,26] but the focus on this study is to determine the isotope effect of (R4) which has implications for the isotopic composition of NO_2, which serves as precursor to atmospheric nitrate.

The kinetic isotope effect associated with (R4) may also play an important role in the $\delta^{15}N$ of NO_2. Previously, $\delta^{15}N$ of NO_x and atmospheric nitrate has been suggested to provide information about NO_x sources.[25–28] Numerous studies have quantified $\delta^{15}N$ from various NO_x sources, and these results indicate that soil emission (denitrification), transportation related sectors, and coal-fired power plants have relatively distinctive $\delta^{15}N$ values.[11–13,25,29–35] These works have motivated several $\delta^{15}N$ studies of atmospheric nitrate as a way to partition NO_x sources to evaluate local/regional changes in NO_x source budgets.[27,28,36] However, the isotopic fractionation processes associated with the photochemical cycling of NO_x such as (R4), NO_2 photolysis, and NO_x isotopic exchange may alter the N isotopic composition of NO and NO_2 relative to total NO_x;[15] however, except for NO_x isotope exchange, these fractionation processes' impact on $\delta^{15}N$ is relatively unknown.[15] If these fractionation processes are significant, daytime $\delta^{15}N$–NO_2 may not equal $\delta^{15}N$–NO_x,[15,16] which has important implications for atmospheric nitrate formed during the daytime, because it is primarily formed through the reaction between NO_2 and photochemically produced $^\bullet OH$.[37] Therefore, it is important to understand the kinetic isotope effect associated with (R4) and its implications for $\delta^{15}N$ of daytime produced atmospheric nitrate.

Bigeleisen demonstrated kinetic isotope effects (KIEs) could be approximated for reactions such as (R4) using transition state theory if the vibrational frequencies of the reactants and transition state are known.[38] Unfortunately, transition state frequencies for many isotopologues in NO_x related reactions, such as (R4), are unknown. Previously, *ab initio* methods have been used to calculate the reaction mechanism, thermochemistry, and vibrational frequencies of (R4),[39] but only for the main isotopologues. The present study builds on Ref. 39 by employing *ab initio* methods to calculate nitrogen and position-specific oxygen KIEs associated with (R4). This will allow for an understanding of the impact (R4) has on the $\delta^{18}O$ value of the transferred O atom from O_3 to NO and on $\delta^{15}N$ as NO is oxidized to NO_2.

II. METHODS

The assumed reaction mechanism of (R4) is shown in Fig. 1, which is based on the results from Ref. 39. In the previous study, geometries and vibrational frequencies for all stationary points along the potential energy surface (PES) have been calculated by UHF, UMP2, and UMP4 methods with the 6-31G(d), 6-311G(d), and 6-311G(d,f) basis sets.[39] Unfortunately the UMP2 and UMP4 levels predicted anomalous vibrational frequencies for the radicals NO and NO_2 due to spin contamination and for O_3 due to its multireference character.[39] These inaccurate vibrational frequencies will have a significant impact on the accuracy of the calculated KIEs. Therefore, we have recalculated the geometries for a
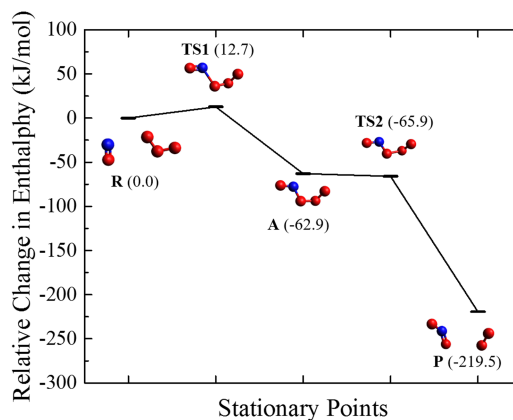
FIG. 1. Schematic diagram of the assumed potential energy curve for the reaction $NO + O_3 \rightarrow NO_2 + O_2$ based on prior calculations using QCISD(T)/ 6-311G(2d)//UMP2(full)/6-31G(d)[39] where **R**, **TS1**, **A**, **TS2**, and **P** refer to the reactants, transition state 1, intermediate, transition state 2, and products, respectively. Relative energies with respect to the reactants $NO + O_3$ are given in kJ/mol and includes ZPE and thermal corrections (298 K).

portion of the potential energy surface (PES) that included the reactants, products, and rate-determining transition state, which has been previously determined to be the NO radical approach to O_3 (**TS1**, Fig. 1),[39] using the high-level quantum mechanical method CCSD(T) with the 6-31G(d) and 6-311G(d) basis sets. The reactants and products geometry optimizations were carried out using default convergence criteria, while **TS1** was optimized from calculated force constants at the previously reported UMP2(full)/6-31G(d) geometry.[39] Vibrational frequency analysis was performed to confirm that the obtained structures are stationary points along the PES that correspond to either a local minimum (3n-6 or 3n-5 real normal modes of vibration) or a transition state (exactly one imaginary frequency). Systematic model errors in the calculated harmonic frequencies have been accounted for by applying a constant scale factor of 0.9899 and 0.9542 for CCSD(T)/6-31G(d) and CCSD(T)/6-311G(d), respectively (Fig. S1 of the supplementary material). All calculations were performed with the Gaussian09 program package revision D.01[40] on the Purdue Radon cluster.[41]

Nitrogen and position-specific oxygen KIEs were calculated in accordance with the Born-Oppenheimer, rigid-rotor, and harmonic approximations, using the complete Bigeleisen equations[38] as implemented in the ISOEFF program[42] at 220, 250, 273, 298, and 320 K. Both the Bigeleisen equations and the ISOEFF program define the calculated KIE as the ratio of reaction coefficients of the light to heavy isotope. However, since we are interested in the relative rate of the heavy to light isotope, we report all calculated KIEs as the ratio of the heavy to the light isotope,

$$KIE = \alpha = \frac{k_H}{k_L} \qquad (2)$$

where α is the calculated KIE, which is also referred to as the isotopic fractionation factor, and H and L refer to the heavy and light isotopes of a particular isotopologue pair, respectively. Corrections for tunneling and anharmonicity were neglected as these isotope effects tend to be small[43] and tend to cancel each other out for heavy atoms as anharmonicity tends to lower the magnitude of the calculated KIE while tunneling

tends to increase the magnitude of the calculated KIE.[44] Additionally, neglect of tunnel effects may be validated due to the involved heavy atoms[45] and the observed low frequency modes along the reaction coordinate. The activation entropy ($\Delta S^{\ddagger}$) for this reaction is negative (-28.7 and -30.6 Cal*Mol^{-1}*K^{-1} for CCSD(T)/6-31G(d) and CCSD(T)/6-311G(d)), so that the reaction is characterized by a "tight transitions state,"[46] which should satisfy the rigid-rotor approximation used within the Bigeleisen equations. Overall, we expect the assumed approximations in to have a minimal impact on the calculated KIEs while pointing out that the calculated KIEs are an approximation.

III. RESULTS AND DISCUSSION

A. Calculated geometries and vibrational frequencies

Table I compares the geometries and harmonic frequencies for the most abundant isotopologues of NO, O_3, NO_2, and O_2 calculated by CCSD(T)/6-31G(d) and CCSD(T)/6-311G(d) with experimental data.[47–54] Overall, the calculated geometries for the reactants and products are in excellent agreement with experimental data, as calculated bond lengths and bond angles are within 0.023 Å and 0.4° of experimental data[49,52,54] (Table I). Additionally, the calculated harmonic frequencies (scaled) are within a maximum difference of 92.2 cm^{-1} and an average error of 29.9 cm^{-1} and 43.9 cm^{-1} relative to experimental data[47,48,50,51] at CCSD(T)/6-31G(d) and CCSD(T)/6-311G(d), respectively. Cartesian coordinates of the optimized geometries and the scaled harmonic frequencies calculated for the major isotopologue of NO, O_3, NO_2, and O_2 from CCSD(T)-631G(d) and CCSD(T)/6-311G(d) computed

TABLE I. Calculated and experimental geometries and vibrational frequencies (cm^{-1}) of reactants and products calculated at CCSD(T)/6-31G(d) and CCSD(T)/6-311G(d). Bonds and angles are given in degrees and angstroms, respectively.

Parameter	CCSD(T)/ 6-31G(d)	CCSD(T)/ 6-311G(d)	Expt.
NO			
r(N–O)	1.169	1.154	1.154[54]
ν_1	1947.7	1996.3	1904.1[48]
O_3			
r(O–O)	1.296	1.276	1.278[49]
<O–O–O	116.5	116.9	116.8[49]
ν_1	1106.8	1095.5	1103.2[51]
ν_2	679.3	687.0	701.4[51]
ν_3	984.3	988.2	1042.1[51]
NO_2			
r(N–O)	1.216	1.202	1.193[49]
<O–N–O	133.7	134.0	134.1[49]
ν_1	1333.4	1317.5	1355.9[50]
ν_2	723.1	697.3	756.8[50]
ν_3	1701.6	1697.7	1663.5[50]
O_2			
r(O–O)	1.229	1.210	1.208[52]
ν_1	1562.7	1528.9	1580.4[47]

TABLE II. Comparison of calculated ZPE (cm^{-1}) using fundamental frequencies derived from experimental data, and calculated using scaled CCSD(T)/6-31G(d), and CCSD(T)/6-311G(d) frequencies. The relative difference in the ZPE (ΔZPE) for the minor isotopologues relative to the most abundant is shown in parentheses (cm^{-1}).[a]

	ZPE		
	Experiment	CCSD(T)/ 6-31G(d)	CCSD(T)/ 6-311G(d)
^{14}N^{16}O	953.9[48]	975.8	1000.1
^{15}N^{16}O	936.9 (17.1)[48]	958.4 (17.4)	982.3 (17.9)
^{14}N^{18}O	928.8 (25.1)[b]	950.1 (25.7)	973.8 (26.3)
^{16}O^{16}O^{16}O	1425.9[53]	1388.0	1388.2
^{18}O^{16}O^{16}O	1404.3 (21.6)[53]	1366.2 (21.7)	1366.5 (21.7)
^{16}O^{18}O^{16}O	1390.8 (35.1)[53]	1352.9 (35.1)	1352.9 (35.2)
^{14}N^{16}O^{16}O	1871.3* [55]	1882.8	1860.0
^{15}N^{16}O^{16}O	1841.3 (30.0)* [55]	1852.2 (30.6)	1830.3 (29.7)
^{14}N^{18}O^{16}O	1844.0 (27.3)* [55]	1855.3 (27.5)	1830.3 (29.7)
^{16}O^{16}O	791.8[47]	782.9	766.0
^{18}O^{16}O	769.2 (22.5)[b]	760.8 (22.1)	744.4 (21.6)

[a]ZPE is calculated as $\frac{1}{2}h\sum \nu_i$ except for the values marked with asterisks in which experimentally derived ZPEs are reported.
[b]Calculated from $\nu = \frac{1}{2\pi}\sqrt{\frac{k}{\mu}}$.

force constants are available in the supplementary material (Tables S1 and S2).

An important point in accurately calculating KIEs is accounting for relative changes in vibrational energies due to substitution of a heavier isotope. Table II compares the differences in calculated vibrational zero point energies (ZPE = $^1/_2 h\sum \nu_i$) for various reactant and product ^{15}N and ^{18}O isotopologues relative to the major isotopologues for CCSD(T)/6-31G(d) and CCSD(T)/6-311G(d) with available experimental data.[47,48,53,55] The difference in vibrational energies for each minor isotopologues relative to the most abundant is shown in parentheses in Table II. Our calculated relative difference in ZPE due to substitution of a heavier isotope is within 1.2 cm^{-1} of experimental data and an average relative difference of 0.34 and 0.61 cm^{-1} for CCSD(T)/6-31G(d) and CCSD(T)/6-311G(d), respectively (Table II). This comparison shows the ability of our chosen level of theories to accurately reproduce changes in ZPE due to isotopic substitution. Therefore, CCSD(T)/6-31G(d) and CCSD(T)/6-311G(d) should be sufficient methods to calculate the relative changes in thermodynamic properties of the N and O isotopologues necessary to determine the KIEs of (R4).

The calculated geometries of **TS1** and atom labeling scheme is displayed in Fig. 2. As expected for an exothermic reaction, **TS1** shows very small perturbations of geometrical parameters relative to the reactants.[56] Except for O_4, the atoms of **TS1** are nearly planar as evident from the dihedral angle <(O_1–N_1–O_2–O_3) of $-169.6°$ and $-171.3°$ at CCSD(T)/6-31G(d) and CCSD(T)/6-311G(d), respectively (Fig. 2), which is a similar finding to geometry of **TS1** calculated at the UMP2/6-31(d) level of theory.[39] The imaginary frequency corresponding to the reaction coordinate is calculated to be 337.5i and 335.1i for CCSD(T)/6-31G(d) and CCSD(T)/6-311G(d), respectively, which is in close agreement with the previous calculated value of 352.9i at UMP2/6-31G(d).[39] Cartesian
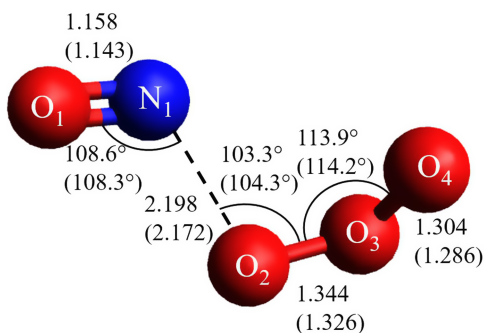
FIG. 2. Optimized geometry of TS1 at CCSD(T)/6-31G(d) and CCSD(T)/6-311G(d) (given in parentheses). Bond lengths are in Angstroms and angles are in degrees. The dihedral angles of TS1 <(O_1–N_1–O_2–O_3) and <(N_1–O_2–O_3–O_4) are −169.6° (−171.3°) and 77.8° (78.6°), respectively.

coordinates of the optimized geometries and the scaled harmonic frequencies calculated for the major isotopologues of **TS1** from CCSD(T)-631G(d) and CCSD(T)/6-311G(d) computed force constants are available in the supplementary material (Tables S3 and S4).

B. Calculated kinetic isotope effects

Calculated nitrogen and position-specific oxygen α values at 298 K are reported in Table III as isotopic enrichment factors in units of per mil (‰),

$$\varepsilon(‰) = 1000\,(\alpha - 1). \qquad (3)$$

Both the CCSD(T)/6-31G(d) and CCSD(T)/6-311G(d) methods calculate similar $\varepsilon(‰)$ values that differed by no more than 1.6‰ (Table III). The largest KIE is observed to occur for the substitution of ^{18}O along the reaction coordinate (the ON + ^{18}OOO → ON^{18}O + OO) that is calculated to be −43.9 and −44.7‰ using CCSD(T)/6-31G(d) and CCSD(T)/6-311G(d) calculated frequencies, respectively (Table III). The magnitude of the KIE is observed to decrease as the isotopic substitution position is further away for the reaction coordinate (i.e., secondary KIEs) as expected (Table III). Isotopic enrichment factors have also been calculated at 220, 250, 273, and 320 K and are provided in the supplementary material (Tables S5 and S6). It is important to note that we cannot claim perfection in these calculated KIEs due to numerous uncertainties associated with transition state theory (e.g.,

TABLE III. Calculated isotopic enrichment factors at CCSD(T)/6-31G(d) and CCSD(T)/6-311G(d) expressed in units of per mil (‰) at 298 K.

	$\varepsilon(‰)$	
Reaction	CCSD(T)/ 6-31G(d)	CCSD(T)/ 6-311G(d)
ON + ^{18}OOO → ON^{18}O + OO	−43.9	−44.7
ON + ^{17}OOO → ON^{17}O + OO	−23.3	−23.7
ON + O^{18}OO → ONO + ^{18}OO	−12.7	−14.1
O^{15}N + OOO → O^{15}NO + OO	−7.7	−6.7
ON + O^{17}OO → ONO + ^{17}OO	−6.7	−7.4
^{17}ON + OOO → ^{17}ONO + OO	0.2	−0.6
^{18}ON + OOO → ^{18}ONO + OO	0.3	−1.3
ON + OO^{17}O → ONO + O^{17}O	0.4	−0.2
ON + OO^{18}O → ONO + O^{18}O	0.8	−0.3

unknown tunneling effects, rigid-rotor and harmonic oscillator approximations) and the computational limitations (e.g., incomplete basis sets, uncertainties in the predicted transition state geometry). Despite these uncertainties, the excellent agreement between predicted geometries, vibrational frequencies, and shifts in ZPEs due to isotopic substitution with experimental data (Tables I and II) lend confidence in the calculated KIEs. Thus, these values should serve as a decent approximation that will be useful for future isotopic modeling of NO$_x$ chemistry.

Oxygen mass-dependent relationships (ln($^{17}\alpha$)/ln($^{18}\alpha$))[23] for position-specific oxygen isotopic substitution are displayed in Table IV. Generally, (ln($^{17}\alpha$)/ln($^{18}\alpha$)) is found to range between 0.524 and 0.527, which is close to the generally accepted value of 0.520.[23] However, (ln($^{17}\alpha$)/ln($^{18}\alpha$)) is found to have an anonymously large deviation from 0.520 for the ^{x}ON + OOO → ^{x}ONO + O$_2$ reaction that is calculated to be 0.7072 and 0.4822 for CCSD(T)/6-31G(d) and CCSD(T)/6-311G(d), respectively (Table V), which occurs due to both $^{18}\alpha$ and $^{17}\alpha$ being close to unity.[57] Despite this deviation, this reaction will have a minimal impact on Δ^{17}O (<0.05‰) as shown in Table IV since both $^{18}\alpha$ and $^{17}\alpha$ are close to unity, where Δ^{17}O is calculated as

$$\Delta^{17}O(‰) = 1000 \ln\left[1 + (^{17}\alpha - 1)\right] - \lambda$$
$$\times 1000 \ln\left[1 + (^{18}\alpha - 1)\right]. \qquad (4)$$

In Eq. (4), λ is assumed to be 0.52.

C. Comparison with experimental data

1. KIE in unreacted O_3

Previously, Ref. 58 experimentally determined the kinetic isotopic fractionation associated with the NO + O$_3$ → NO$_2$ + O$_2$ reaction by reacting NO with excess O$_3$ and measuring the O isotopic composition of the unreacted O$_3$ and reported an overall $\varepsilon(‰)$ of −30.5‰ for ^{18}O. This experimentally determined $\varepsilon(‰)$ value does not correspond to a singular KIE, rather it is roughly a statistical average for all the KIEs associated with the various ^{18}O isotopomers of O$_3$ and their reactions with NO. In order to quantitatively evaluate our calculated KIEs with respect to the results obtained by Ref. 58, we modeled the kinetics for reactions of the various O$_3$ isotopomers with NO using a subset of a previously published NO$_x$ cycle chemical kinetics model,[10] utilizing *Kintecus*, a chemical kinetics compiler.[59]

The NO$_x$ cycling kinetics model previously published by Ref. 10 contains numerous facets of the NO$_x$ cycle including NO$_2$ dissociation, oxygen isotope exchange, ozone formation, ozone dissociation, NO oxidation by O$_3$, NO oxidation by O-atom, NO$_2$ reaction with O-atom, NO$_2$ exchange with O-atom, NO exchange with O-atom, NO$_2$ exchange with NO, and NO oxidation by O$_2$. Here, we are only interested in the KIE associated with the reaction of the various isotopomers of O$_3$ with NO, so only the reactions pertaining to this reaction were used in the present study, which are displayed in Table V. In our model, we have only considered ^{18}O isotopic substitution due to this reaction being a mass-dependent fractionation process. Since we are interested in the relative change of the

TABLE IV. Calculated oxygen mass-dependence relationships ($\ln(^{17}\alpha)/\ln(^{18}\alpha)$) and mass-independence values ($\Delta^{17}O$) at 298 K.

Reaction	$\ln(^{17}\alpha)/\ln(^{18}\alpha)$		$\Delta^{17}O(\permil)$[a]	
	CCSD(T)/6-31G(d)	CCSD(T)/6-311G(d)	CCSD(T)/6-31G(d)	CCSD(T)/6-311G(d)
$^{x}ON + OOO \rightarrow {}^{x}ONO + OO$	0.707	0.482	−0.05	−0.05
$ON + {}^{x}OOO \rightarrow ON^{x}O + OO$	0.524	0.525	0.20	0.21
$ON + O^{x}OO \rightarrow ONO + {}^{x}OO$	0.527	0.527	0.08	0.10
$ON + OO^{x}O \rightarrow ONO + O^{x}O$	0.527	0.526	−0.01	0.02

[a] $\Delta^{17}O(\permil)$ calculated from Eq. (4).

^{18}O isotopic composition of O_3, the starting composition is unimportant, so we specified a starting $\delta^{18}O(O_3)$ of $0\permil$ that was assumed to be uniformly distributed within O_3. While there is experiment evidence that $\delta^{18}O$ is not uniformly distributed within O_3,[60] this should have a minor impact on the relative change of bulk isotopic composition of $\delta^{18}O$ in our model. The reaction of NO with the main isotopologue of O_3 ($^{16}O^{16}O^{16}O$) was set to 1.73×10^{-14} cm^3*molecules^{-1}*s^{-1},[61] and the reactions of NO with the ^{18}O substituted O_3 isotopologues/isotopomers were scaled by their position-specific oxygen α value. Additionally, the reactions involving the asymmetric isotopic substituted O_3 isotopologue (^{18}OOO) were scaled by 0.5 to account for the reaction channel symmetry (Table V). Our model was initiated with a $NO:O_3$ ratio of 0.95:1 so that O_3 was slightly in excess as in the experiment conducted by Ref. 58.

From the model output, a Rayleigh-type distillation curve of the $\delta^{18}O$ of unreacted O_3 was constructed in the form of

$$\ln\left(1 + 0.001 * \delta_f\right) = \ln\left(1 + 0.001 * \delta_0\right) + (\alpha - 1)\ln(f) \quad (5)$$

where δ_f and δ_0 are the initial and final $\delta^{18}O$ of O_3, respectively, and f is the fraction of unreacted O_3. Fig. 3 displays our calculated Rayleigh type distillation curve for O_3, where the slope of the line indicates an $\varepsilon(\permil)$ value of $-18.6\permil$ and $-19.6\permil$ for CCSD(T)/6-31G(d) and CCSD(T)/6-311G(d), respectively, which differs from the experimentally determined value of $-30.5\permil$.[58] However, re-analysis of the experimental data from Ref. 59 indicates that there might be a high-leverage, influential x data point at $\ln(f) = -3.047$. Fig. 4 compares two linear regression models of the experimental data from Ref. 59 which includes all of the data points (model A) and the omission of the data point at $\ln(f) = -3.047$ (model B). While the R^2 values from the two models do not vary by much ($R^2 = 0.966$ and 0.969), the slopes drastically change from -0.0305

± 0.003 to -0.0209 ± 0.003 for model A and model B, respectively (Fig. 4). The calculated $\varepsilon(\permil)$ from model B is $-20.9 \pm 0.003\permil$, which is in excellent agreement with our calculated and modeled value at both CCSD(T)/6-31G(d) and CCSD(T)/6-311G(d). This might suggest that the data point at $\ln(f) = -3.047$ might be influenced by other isotopic fractionation processes such as the formation of higher order nitrogen oxide species such as NO_3 and N_2O_5 that might have a different α. Also, it is also important to point out the limitations in our calculated α values from the Bigeleisen equations that are obtained within the conventional transition state theory with harmonic normal modes and rigid rotor approximations.[38] Additionally, the experimental α may be influenced by the $NO + O_3$ reaction pathway proceeding through the O extraction from the apex O atom position of O_3 that recent experimental data shows may have a branching ratio of $8\% \pm 5\%$, which was neglected in the theoretial α.[8] However, our calculated α values tend to agree quite well with a significant portion of the experimental data.

2. O transfer KIE

Another important KIE to consider is the O transfer during the oxidation of NO by O_3 to NO_2, which will be referred to as $^{18}\varepsilon_{(O\text{-}trans)}$,

$$^{18}\varepsilon_{(O\text{-}trans)}(\permil) = \delta^{18}O(NO_{2(O\text{-}trans)})(\permil) - \delta^{18}O(aO_3)(\permil) \quad (6)$$

TABLE V. Adapted rate constants (k) at 298 K (10^{-14} cm^3 molecules^{-1} s^{-1}) of NO reactions with various O_3 isotopologues using KIEs calculated at CCSD(T)/6-31G(d) and CCSD(T)/6-311G(d).

	k(298 K)	
Reaction	CCSD(T)/ 6-31G(d)	CCSD(T)/ 6-311G(d)
$^{16}O^{14}N + {}^{16}O^{16}O^{16}O \rightarrow {}^{16}O^{14}N^{16}O + {}^{16}O^{16}O$	1.730	1.730
$^{16}O^{14}N + {}^{18}O^{16}O^{16}O \rightarrow {}^{16}O^{14}N^{18}O + {}^{16}O^{16}O$	0.827	0.826
$^{16}O^{14}N + {}^{18}O^{16}O^{16}O \rightarrow {}^{16}O^{14}N^{16}O + {}^{18}O^{16}O$	0.866	0.864
$^{16}O^{14}N + {}^{16}O^{18}O^{16}O \rightarrow {}^{16}O^{14}N^{16}O + {}^{18}O^{16}O$	1.708	1.706

FIG. 3. Rayleigh distillation model of unreacted O_3 in the $NO + O_3$ reaction calculated using KIEs at CCSD(T)/6-31G(d) and CCSD(T)/6-311G(d) within *Kintecus*. The slopes of the linear regression model indicate an overall $\varepsilon(\permil)$ of $-18.6\permil$ and $-19.6\permil$ for unreacted O_3 at CCSD(T)/6-31G(d) and CCSD(T)/6-311G(d), respectively.
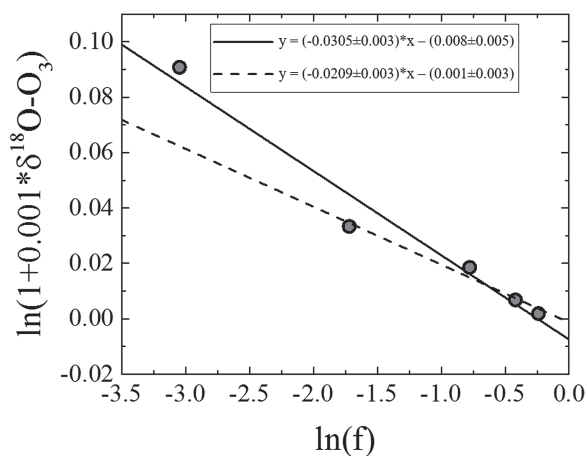
FIG. 4. Rayleigh distillation model of unreacted O_3 in the NO + O_3 reaction calculated using prior experimental data.[58] Inclusion of all experimental data indicate a slope of -0.0305 ± 0.003 that corresponds to an ε(‰) of -30.5 ± 0.003‰ (solid line, $R^2 = 0.966$). Omission of the data point at ln(f) = -3.04 indicates a slope of -0.0209 ± 0.003 that corresponds to an ε(‰) of -20.9 ± 0.003‰ (dashed line, $R^2 = 0.969$).

where $\delta^{18}O(NO_{2(O\text{-}trans)})$ and $\delta^{18}O(aO_3)$ are the $\delta^{18}O$ values of the transferred O atom in NO_2 and asymmetric O_3, respectively. Previously, in Ref. 8, NO reacted with O_3 at a 1:1 ratio at room temperature and the $\delta^{18}O$ of the transferred O atom in NO_2 was measured. Using their experimental data, statistical models of previous studies of the intermolecular isotope distributions of O_3,[62] and the enrichment of asymmetric and symmetric O_3 isotopologues in the stratosphere as a function of altitude,[63] $^{18}\varepsilon_{(O\text{-}trans)}$ was estimated to be -23.9 and -20.8‰.[8] Under the experimental conditions (i.e., 1:1 ratio of NO:O_3), the products, NO_2 and O_2, reflect the partitioning of ^{18}O based on the position-specific α values for the ^{18}O isotopomers of O_3, as there is a minimal isotopic fractionation impacting the residual O_3 since it nearly completely reacts.

Using our *Kintecus* model described in Sec. III C 1, we have estimated the $^{18}\varepsilon_{(O\text{-}trans)}$ using our O_3 isotopologue dependent KIEs and a NO:O_3 ratio of 1:1. The ^{18}O isotopic composition of O_3 was assumed to be uniformly distributed with a starting $\delta^{18}O(O_3) = \delta^{18}O(aO_3) = 0$‰. From the output of our model, we estimate $\delta^{18}O(NO_{2(O\text{-}trans)})$ and thus $^{18}\varepsilon_{(O\text{-}trans)}$ (Eq. (6)) to be -22.8‰ for both CCSD(T)/6-31G(d) and CCSD(T)/6-311G(d) calculated α values, respectively. These values are in excellent agreement with the experimental determined values that are estimated to range between -23.9‰ and -20.8‰.[8]

IV. CONCLUSION

Ab initio calculations have been carried out to investigate the nitrogen and oxygen KIEs associated with NO reaction with O_3. The calculated KIEs were generally close to unity except for primary KIEs, in which relatively large enrichment factors were calculated to be -44.7 and -6.7‰ for the $^{16}O^{14}N + {}^{18}O^{16}O^{16}O \rightarrow {}^{16}O^{14}N^{18}O + {}^{16}O^{16}O$ and $^{16}O^{15}N + {}^{16}O^{16}O^{16}O \rightarrow {}^{16}O^{16}N^{16}O + {}^{16}O^{16}O$ reactions, respectively, at 298 K (CCSD(T)/6-311G(d)). The reported KIEs may be limited due to the approximations used within the Bigeleisen equations and the computational limitations;

however, excellent agreement between predicted geometries, vibrational frequencies, and shifts in ZPE due to isotopic substitution with experimental data suggests that our applied methods should provide a decent KIE approximation. Additionally, kinetic modeling of our calculated oxygen position-specific KIEs indicates the excellent agreement between our values and prior experimental measurements, which indicates that our applied methods are generally capturing the underlying physics correctly. Our calculations indicate that the O mass-dependent relationship ($\ln(^{17}\alpha)/\ln(^{18}\alpha)$) is generally near the expected value of 0.52. Cases in which ($\ln(^{17}\alpha)/\ln(^{18}\alpha)$) deviates from the expected value occur when the calculated KIEs are close to unity and thus have a minor impact on $\Delta^{17}O$, as expected for a mass-dependent fractionation process. This indicates that NO reaction with O_3 may play a significant role in the $\delta^{15}N$ and $\delta^{18}O$ values of NO and NO_2, without altering $\Delta^{17}O$. This has important implications for utilizing $\delta^{15}N$ and $\delta^{18}O$ as tools for NO_x source partitioning and for understanding NO_x photochemical cycling. The calculated KIEs will be useful for future work aimed at modeling NO_x isotope chemistry and will help guide future ambient NO_x isotopic measurements. Additionally, future work should aim to estimate the branching ratio of the NO reaction with O_3 at the apex O-atom position using *ab initio* methods.

SUPPLEMENTARY MATERIAL

See supplementary material for harmonic frequency scale factors, Cartesian coordinates for all calculated stationary points, calculated isotopologue harmonic frequencies, and calculated temperature dependent KIEs.

[1]P. Leighton, *Photochemistry of Air Pollution* (Academic, New York, 1961).
[2]P. J. Crutzen, *Gas-Phase Nitrogen and Methane Chemistry in the Atmosphere* (D. Reidel Publishing Company, Dordrecht, Holland, 1973).
[3]P. J. Crutzen, Annu. Rev. Earth Planet. Sci. **7**, 443 (1979).
[4]J. A. Logan, J. Geophys. Res.: Oceans **88**, 10785, doi:10.1029/JC088iC15p10785 (1983).
[5]B. J. Finlayson-Pitts and J. N. Pitts Jr., *Chemistry of the Upper and Lower Atmosphere: Theory, Experiments, and Applications* (Academic Press, 1999).
[6]G. Michalski, Z. Scott, M. Kabiling, and M. H. Thiemens, Geophys. Res. Lett. **30**, 1870, doi:10.1029/2003gl017015 (2003).
[7]S. Morin, J. Savarino, M. M. Frey, N. Yan, S. Bekki, J. W. Bottenheim, and J. M. Martins, Science **322**, 730 (2008).
[8]J. Savarino, S. K. Bhattacharya, S. Morin, M. Baroni, and J.-F. Doussin, J. Chem. Phys. **128**, 194303 (2008).
[9]G. Michalski, S. K. Bhattacharya, and D. F. Mase, in *Handbook of Environmental Isotope Geochemistry* (Springer, 2012), pp. 613–635.
[10]G. Michalski, S. K. Bhattacharya, and G. Girsch, Atmos. Chem. Phys. **14**, 4935 (2014).
[11]H. Moore, Atmos. Environ. **1967**(11), 1239 (1977).

[12]D. L. Fibiger, M. G. Hastings, A. F. Lew, and R. E. Peltier, Anal. Chem. **86**, 12115 (2014).

[13]W. W. Walters, B. D. Tharp, H. Fang, B. J. Kozak, and G. Michalski, Environ. Sci. Technol. **19**, 11363 (2015).

[14]H. D. Freyer, D. Kley, A. Volz-Thomas, and K. Kobel, J. Geophys. Res. **98**, 14791, doi:10.1029/93JD00874 (1993).

[15]W. W. Walters, D. S. Simonini, and G. Michalski, Geophys. Res. Lett. **43**, 440, doi:10.1002/2015GL066438 (2016).

[16]W. W. Walters and G. Michalski, Geochim. Cosmochim. Acta **191**, 89 (2016).

[17]M. H. Thiemens and J. E. Heidenreich, Science **219**, 1073 (1983).

[18]D. Krankowsky, F. Bartecki, G. G. Klees, K. Mauersberger, K. Schellenbach, and J. Stehr, Geophys. Res. Lett. **22**, 1713, doi:10.1029/95gl01436 (1995).

[19]J. C. Johnston and M. H. Thiemens, J. Geophys. Res.: Atmos. **1984–2012**(102), 25395, doi:10.1029/97JD02075 (1997).

[20]K. Mauersberger, P. Lämmerzahl, and D. Krankowsky, Geophys. Res. Lett. **28**, 3155, doi:10.1029/2001GL013439 (2001).

[21]W. C. Vicars, S. K. Bhattacharya, J. Erbland, and J. Savarino, Rapid Commun. Mass Spectrom. **26**, 1219 (2012).

[22]W. C. Vicars and J. Savarino, Geochim. Cosmochim. Acta **135**, 270 (2014).

[23]M. F. Miller, Geochim. Cosmochim. Acta **66**, 1881 (2002).

[24]M. H. Thiemens, Annu. Rev. Earth Planet. Sci. **34**, 217 (2006).

[25]T. H. E. Heaton, Atmos. Environ. **1967**(21), 843 (1987).

[26]H. D. Freyer, Tellus, Ser. B **43**, 30 (1991).

[27]E. M. Elliott, C. Kendall, S. D. Wankel, D. A. Burns, E. W. Boyer, K. Harlin, D. J. Bain, and T. J. Butler, Environ. Sci. Technol. **41**, 7661 (2007).

[28]E. M. Elliott, C. Kendall, E. W. Boyer, D. A. Burns, G. G. Lear, H. E. Golden, K. Harlin, A. Bytnerowicz, T. J. Butler, and R. Glatz, J. Geophys. Res.: Biogeosci. **114**, G04020, doi:10.1029/2008JG000889 (2009).

[29]T. Hoering, Geochim. Cosmochim. Acta **12**, 97 (1957).

[30]T. H. E. Heaton, Tellus, Ser. B **42**, 304 (1990).

[31]D. Li and X. Wang, Atmos. Environ. **42**, 4747 (2008).

[32]J. D. Felix, E. M. Elliott, and S. L. Shaw, Environ. Sci. Technol. **46**, 3528 (2012).

[33]J. D. Felix and E. M. Elliott, Geophys. Res. Lett. **40**, 1642, doi:10.1002/grl.50209 (2013).

[34]J. D. Felix and E. M. Elliott, Atmos. Environ. **92**, 359 (2014).

[35]W. W. Walters, S. R. Goodwin, and G. Michalski, Environ. Sci. Technol. **49**, 2278 (2015).

[36]F. Beyn, V. Matthias, A. Aulinger, and K. Dähnke, Atmos. Environ. **107**, 281 (2015).

[37]J. G. Calvert, A. Lazrus, G. L. Kok, B. G. Heikes, J. G. Walega, J. Lind, and C. A. Cantrell, Nature **317**, 27 (1985).

[38]J. Bigeleisen, J. Chem. Phys. **17**, 675 (1949).

[39]J. Peiró-García and I. Nebot-Gil, J. Phys. Chem. A **106**, 10302 (2002).

[40]M. J. Frisch, G. W. Trucks, H. B. Schlegel, G. E. Scuseria, M. A. Robb, J. R. Cheeseman, G. Scalmani, V. Barone, B. Mennucci, G. A. Petersson, H. Nakatsuji, M. Caricato, X. Li, H. P. Hratchian, A. F. Izmaylov, J. Bloino, G. Zheng, J. L. Sonnenberg, M. Hada, M. Ehara, K. Toyota, R. Fukuda, J. Hasegawa, M. Ishida, T. Nakajima, Y. Honda, O. Kitao, H. Nakai, T. Vreven, J. A. Montgomery, Jr., J. E. Peralta, F. Ogliaro, M. Bearpark, J. J. Heyd, E. Brothers, K. N. Kudin, V. N. Staroverov, R. Kobayashi, J. Normand, K. Raghavachari, A. Rendell, J. C. Burant, S. S. Iyengar, J. Tomasi, M. Cossi, N. Rega, J. M. Milliam, M. Klene, J. E. Knox, J. B. Cross, V. Bakken, C. Adamo, J. Jaramillo, R. Gomperts, R. E. Stratmann, O. Yazyev, A. J. Austin, R. Cammi, C. Pomelli, J. W. Ochterski, R. L. Martin, K. Morokuma, V. G. Zakrzewski, G. A. Voth, P. Salvador, J. J. Dannenberg, S. Dapprich, A. D. Daniels, Ö. Farkas, J. B. Foresman, J. V. Ortiz, J. Cioslowski, and D. J. Fox, GAUSSIAN 09, Revision D.01, Gaussian, Inc., Wallingford, CT, 2009.

[41]Purdue Radon Cluster web url: https://www.rcac.purdue.edu/compute/radon/ (last accessed April 4, 2015).

[42]V. Anisimov and P. Paneth, J. Math. Chem. **26**, 75 (1999).

[43]R. E. Weston, Chem. Rev. **99**, 2115 (1999).

[44]P. Adamczyk, A. Dybala-Defratyka, and P. Paneth, Environ. Sci. Technol. **45**, 3006 (2011).

[45]L. C. Melander and W. H. Saunders, Reaction Rates of Isotopic Molecules (John Wiley & Sons, 1980).

[46]T. Baer and W. L. Hase, Unimolecular Reaction Dynamics: Theory and Experiments (Oxford University Press on Demand, 1996).

[47]H. D. Babcock and L. Herzberg, Astrophys. J. **108**, 167 (1948).

[48]M. D. Olman, M. D. McNelis, and C. D. Hause, J. Mol. Spectrosc. **14**, 62 (1964).

[49]G. Hertzberg, Electronic Spectra and Electronic Structure of Polyatomic Molecules (Van Nostrand, New York, 1966).

[50]R. E. Blank and C. D. Hause, J. Mol. Spectrosc. **34**, 478 (1970).

[51]T. Shimanouchi, J. Phys. Chem. Ref. Data **6**, 993 (1977).

[52]K. P. Huber and G. Herzberg, in Molecular Spectra and Molecular Structure. IV. Constants of Diatomic Molecules (Van Nostrand Reinhold Co., 1979), pp. 8–689.

[53]J. I. Steinfeld, S. M. Adler-Golden, and J. W. Gallagher, J. Phys. Chem. Ref. Data **16**, 911 (1987).

[54]F. J. Lovas, E. Tiemann, J. S. Coursey, S. A. Kotochigova, J. Chang, K. Olsen, and R. A. Dragoset, Phys. Ref. Data http://www.nist.gov/pml/data/msd-di/index.cfm (last accessed November 22, 2015).

[55]G. Michalski, R. Jost, D. Sugny, M. Joyeux, and M. Thiemens, J. Chem. Phys. **121**, 7153 (2004).

[56]G. S. Hammond, J. Am. Chem. Soc. **77**, 334 (1955).

[57]T. Otake, A. C. Lasaga, and H. Ohmoto, Chem. Geol. **249**, 357 (2008).

[58]S. Chakraborty and S. Chakraborty, Curr. Sci. **85**, 1210 (2003).

[59]J. C. Ianni, Kintecus V5.5 (2014).

[60]C. Janssen, J. Geophys. Res.: Atmos. **110**, 1984–2012, doi:10.1029/2004JD005479 (2005).

[61]R. Atkinson, D. L. Baulch, R. A. Cox, J. N. Crowley, R. F. Hampson, R. G. Hynes, M. E. Jenkin, M. J. Rossi, and J. Troe, Atmos. Chem. Phys. **4**, 1461 (2004).

[62]S. K. Bhattacharya, A. Pandey, and J. Savarino, J. Geophys. Res.: Atmos. **113**, 1984–2012, doi:10.1029/2006JD008309 (2008).

[63]M.-C. Liang, F. W. Irion, J. D. Weibel, C. E. Miller, G. A. Blake, and Y. L. Yung, J. Geophys. Res.: Atmos. **111**, 9025, doi:10.1029/2005JD006342 (2006).